

Library Copy  
R.A. A72 L 211 R.01

UNCLASSIFIED

Copy 44  
RM SL57E06

12

~~CONFIDENTIAL~~  
**NACA**

# RESEARCH MEMORANDUM

for the

U. S. Air Force

INVESTIGATION OF STATIC STABILITY AND DRAG CHARACTERISTICS  
OF A 1/10-SCALE MODEL OF THE AVCO BOOSTER VEHICLE  
AT MACH NUMBERS OF 1.60 AND 2.00

COORD. NO. AF-AM-58

By James D. Church and Lawrence M. Sista

Langley Aeronautical Laboratory  
Langley Field, Va.

**LIBRARY COPY**

MAY 24 1957

LANGLEY AERONAUTICAL LABORATORY  
LIBRARY, NACA  
LANGLEY FIELD, VIRGINIA

CLASSIFIED DOCUMENT

This material contains information affecting the National Defense of the United States within the meaning of the espionage laws, Title 18, U.S.C., Secs. 793 and 794, the transmission or revelation of which in any manner to an unauthorized person is prohibited by law.

To  
by  
**NATIONAL ADVISORY COMMITTEE  
FOR AERONAUTICS**

WASHINGTON

MAY 10 1957

CLASSIFICATION CHANGED

~~CONFIDENTIAL~~

Priority of *TOP SECRET* Date *2/11/58*

CLASSIFICATION CHANGED

*REMOVED FROM FILE*  
*2/11/58*

~~CONFIDENTIAL~~



## NATIONAL ADVISORY COMMITTEE FOR AERONAUTICS

## RESEARCH MEMORANDUM

for the

U. S. Air Force

## INVESTIGATION OF STATIC STABILITY AND DRAG CHARACTERISTICS

OF A 1/10-SCALE MODEL OF THE AVCO BOOSTER VEHICLE

AT MACH NUMBERS OF 1.60 AND 2.00

COORD. NO. AF-AM-58

By James D. Church and Lawrence M. Sista

## SUMMARY

An investigation has been conducted in the Langley Unitary Plan wind tunnel to determine the static stability and drag characteristics of a 1/10-scale model of the AVCO booster vehicle. The tests were made at a constant Reynolds number, based on maximum nose diameter, of  $1.09 \times 10^6$  at Mach numbers of 1.60 and 2.00.

## INTRODUCTION

At the request of the U. S. Air Force, an investigation of the static stability and drag characteristics of a 1/10-scale model of the AVCO booster vehicle has been conducted by the National Advisory Committee for Aeronautics. The purpose of the full-scale AVCO tests is to accelerate various nose shapes to supersonic Mach numbers, at which point, the nose is to be separated from the booster. Inasmuch as previous transonic-wind-tunnel results indicated that the two bodies might not separate positively, additional wind-tunnel tests were urgently needed to determine the separation forces at expected flight velocities and attitudes.

The present results were obtained at Mach numbers of 1.60 and 2.00 for angles of attack from  $-4^\circ$  to  $12^\circ$  and for various distances separating the nose and the booster. Also included are some effects of Reynolds number, roll position of the stabilizing fins, and booster drag scoops.

~~CONFIDENTIAL~~

## SYMBOLS

The results of these tests are presented as coefficients of forces and moments referred to the body-axis system. The moments are taken about the center-of-gravity locations illustrated in figure 1.

- $C_A$  axial-force coefficient of complete model,  $\frac{\text{Total axial force}}{qS}$
- $C_{AB}$  axial-force coefficient of booster in presence of nose,  
 $\frac{\text{Booster axial force}}{qS}$
- $C_{AN}$  axial-force coefficient of nose in presence of booster,  
 $\frac{\text{Nose axial force}}{qS}$
- $C_l$  rolling-moment coefficient of complete model,  
 $\frac{\text{Total rolling moment}}{qSD}$
- $C_m$  pitching-moment coefficient of complete model about center  
of gravity of combination,  $\frac{\text{Total pitching moment}}{qSD}$
- $C_{mB}$  pitching-moment coefficient of booster in presence of nose  
about booster center of gravity,  $\frac{\text{Booster pitching moment}}{qSD}$
- $C_{mN}$  pitching-moment coefficient of nose in presence of booster  
about nose center of gravity,  $\frac{\text{Nose pitching moment}}{qSD}$
- $C_N$  normal-force coefficient of complete model,  $\frac{\text{Total normal force}}{qS}$
- $C_{NB}$  normal-force coefficient of booster in presence of nose,  
 $\frac{\text{Booster normal force}}{qS}$
- $C_{NN}$  normal-force coefficient of nose in presence of booster,  
 $\frac{\text{Nose normal force}}{qS}$

$$C_{m\alpha} = \frac{\partial C_m}{\partial \alpha}$$

$$C_{N\alpha} = \frac{\partial C_N}{\partial \alpha}$$

$C_{p1}$  booster rear-cavity pressure coefficient,  $\frac{p_1 - p}{q}$

$C_{p2}$  booster forward-cavity pressure coefficient,  $\frac{p_2 - p}{q}$

$C_{p3}$  nose-cavity pressure coefficient,  $\frac{p_3 - p}{q}$

$C_{p4}$  nose-cone static-pressure coefficient,  $\frac{p_4 - p}{q}$

$C_{p5}$  nose-shoulder base-pressure coefficient,  $\frac{p_5 - p}{q}$

D maximum diameter of nose, 6.00 in.

d distance separating nose and booster (see fig. 1), in.

M Mach number

p free-stream static pressure, lb/sq ft

q free-stream dynamic pressure,  $0.7\rho M^2$ , lb/sq ft

R Reynolds number based on maximum nose diameter

S maximum cross-sectional area of nose,  $\pi D^2/4$ , 0.1964 sq ft

$\alpha$  angle of attack of model center line, deg

$\phi$  roll angle of stabilizing fins (zero angle is position where fins are at  $45^\circ$  with respect to the model normal-force plane), deg

**Subscript:**

meas measured value

## APPARATUS AND MODEL

### Tunnel

The tests were conducted in the low Mach number test section of the Langley Unitary Plan wind tunnel. This tunnel is of the variable-pressure, continuous-flow type with a test section measuring 4 feet square and approximately 7 feet in length. Mach number may be varied continuously from about 1.5 to 2.9 by means of an asymmetric sliding-block nozzle.

### Model and Support System

The 1/10-scale model was constructed of steel and aluminum and was supplied by the Beech Aircraft Corporation. A sketch of the model is presented in figure 1. A photograph of the model with open scoops,  $d = 0.52$  inch, and  $\phi = 0^\circ$  is presented as figure 2.

The nose of the model was fastened to the booster by an internally mounted, NACA three-component, electrical strain-gage balance. The booster-nose assembly was in turn connected to a sting by means of a similar NACA four-component balance. Finally the sting was attached to a remotely operated adjustable-angle coupling. This adjustable coupling, which was mounted in the tunnel central support system, was used in this test to vary the model angle of attack.

Wedge-shaped tabs were mounted on the booster fins to provide spin for stabilization. These stabilizing fins were in turn fastened to the booster shell. Rotation of the fins from their normal ( $\phi = 0^\circ$ ) position was accomplished by rolling the booster shell with respect to the booster-nose assembly. Separation distance was varied by a spring loaded device which translated the booster shell downstream with respect to the nose.

Further details of the tunnel and model support systems may be found in reference 1.

## MEASUREMENTS AND ACCURACY

### Measurements

Stability tests were made through an angle-of-attack range from approximately  $-4^\circ$  to  $12^\circ$  for the complete model with closed scoops ( $d = 0.04$  inch) and from  $-4^\circ$  to  $8^\circ$  for the open-scoop separation studies. All angles of attack were corrected for deflection of the sting and balance under static load conditions. The complete-model stability tests

~~CONFIDENTIAL~~

were conducted for two roll positions of the stabilizing fins, whereas the separation investigation utilized the  $\phi = 0^\circ$  position only.

Measurements for all configurations were recorded at Mach numbers of 1.60 and 2.00 for a Reynolds number of  $1.09 \times 10^6$ . In addition, data for the open-scoop ( $d = 0.04$  inch) configuration at  $M = 2.00$  were obtained for a Reynolds number of  $0.29 \times 10^6$ . The force- and moment-coefficient increments caused by changing the Reynolds number from  $0.29 \times 10^6$  to  $1.09 \times 10^6$  at  $M = 2.00$  for the open-scoop configuration (fig. 3(a)) were assumed to apply to the closed-scoop configuration. In this manner, an approximation of the effect of Reynolds number on the complete-model summary data was obtained.

Stagnation pressure was varied from 8 pounds per square inch to  $9\frac{1}{2}$  pounds per square inch in order to maintain constant Reynolds numbers at a stagnation temperature of approximately  $125^\circ$  F.

At the request of the contractor, the nose-balance axial-force data have been adjusted to correspond to the zero balance-chamber axial-force coefficient as follows:

$$C_{AN} = (C_{AN})_{\text{meas}} + \frac{0.0108}{S} C_{p3}$$

This adjustment results in a conservative estimate of  $C_{AB} - C_{AN}$ , since the pressure acting at the rear of the nose  $C_{p2}$  produces a nose thrusting force if the cavity is partly or completely closed off on the full-scale configuration.

A study of the force data in conjunction with the schlieren photographs indicates wall-reflected shock waves striking the model at  $M = 1.60$  for angles of attack larger than  $5^\circ$  and for all separation distances equal to or less than 0.5 inch. These data indicate that, for separation distances of 0.04 or 0.08 inch, the results are questionable because of the effect of these shock reflections. However, these data have been presented (as flagged symbols) in instances where these effects appeared relatively minor.

#### Accuracy

The tunnel, as yet, has not been completely calibrated and, hence, any flow angularity that might exist in the test section has not been determined. Tunnel pressure gradients in the region of the model have

been determined and are sufficiently small so as not to induce any buoyancy effect on the model.

The accuracy of the presented data based on a knowledge of balance calibration, reproducibility of data, and tunnel calibration is estimated to be within the following limits:

M	.....	±0.015
$\alpha$ , deg	.....	±0.1
$C_N$ , $C_{NB}$	.....	±0.02
$C_A$ , $C_{AB}$	.....	±0.02
$C_m$ , $C_{mB}$	.....	±0.04
$C_L$	.....	±0.004
$C_{NN}$	.....	±0.02
$C_{AN}$	.....	±0.01
$C_{mN}$	.....	±0.01

PRESENTATION OF RESULTS

The results of the investigation are presented in the following figures:

	Figure
Effect of Reynolds number at $M = 2.00$ ; open scoop, $d = 0.04$ inch, and $\phi = 0^\circ$ .....	3
Effect of roll position of stabilizing fins for complete model; scoops closed and $R = 1.09 \times 10^6$ .....	4
Variation with Mach number of complete-model pitch characteristics; closed scoops and $\phi = 0^\circ$ .....	5
Effect of separation distance on booster characteristics; scoops open, $\phi = 0^\circ$ , and $R = 1.09 \times 10^6$ .....	6
Effect of separation distance on nose characteristics; scoops open, $\phi = 0^\circ$ , and $R = 1.09 \times 10^6$ .....	7
Variation with separation distance of zero-angle-of-attack axial-force coefficients; $\phi = 0^\circ$ .....	8
Variation with angle of attack of pressure coefficients; $\phi = 0^\circ$ and $R = 1.09 \times 10^6$ .....	9
Variation with separation distance of zero-angle-of-attack pressure coefficients; $\phi = 0^\circ$ .....	10

	Figure
Schlieren photographs of model at two Mach numbers; $\alpha = 0^\circ, \phi = 0^\circ$ . . . . .	11
Schlieren photographs of model at two Mach numbers; $\alpha = 8^\circ, \phi = 0^\circ$ . . . . .	12

RESULTS

The results are presented without analysis; however, some general observations relative to the data are as follows:

1. The complete model (closed scoops) is statically stable at Mach numbers of 1.6 and 2.0. The stability is relatively unaffected by roll position of the stabilizing fins.

2. At  $M = 2.00$ , a Reynolds number change from  $0.29 \times 10^6$  to  $1.09 \times 10^6$  materially alters the zero-angle-of-attack drag ( $C_{A\alpha=0}$ ) and rolling-moment coefficients, whereas the longitudinal stability appears unaffected. Other low Reynolds number data indicate that the effect on  $C_{A\alpha=0}$  may exist over the entire supersonic Mach number range.

3. Opening the booster scoops appreciably increases the booster drag minus the nose drag for the minimum separation distance at  $M = 1.60$  and 2.00.

4. The static value of the booster drag minus the nose drag becomes negative for separation distances larger than 2.3 inches for both Mach numbers tested. However, the dynamic separation characteristics may be materially different from the static condition because of a proposed nose thrust ejector and existing mass differences between nose and booster.

Langley Aeronautical Laboratory,  
National Advisory Committee for Aeronautics,  
Langley Field, Va., April 10, 1957.

*James D. Church*  
James D. Church  
Aeronautical Research Engineer  
*Lawrence M. Sista*  
Lawrence M. Sista  
Aeronautical Research Engineer

Approved: *Herbert A. Wilson*  
Herbert A. Wilson  
Chief of Unitary Plan Wind Tunnel

jbb

## REFERENCES

1. Anon.: Manual for Users of the Unitary Plan Wind Tunnel Facilities of the National Advisory Committee for Aeronautics. NACA, 1956.
2. Edgar, J. M., and Soderberg, L. R.: Analysis of Transonic Wind-Tunnel Test of a 1/10 Scale AVCO Booster Model. Beech Aerod. Rep. 526, Beech Aircraft Corp., May 1956.

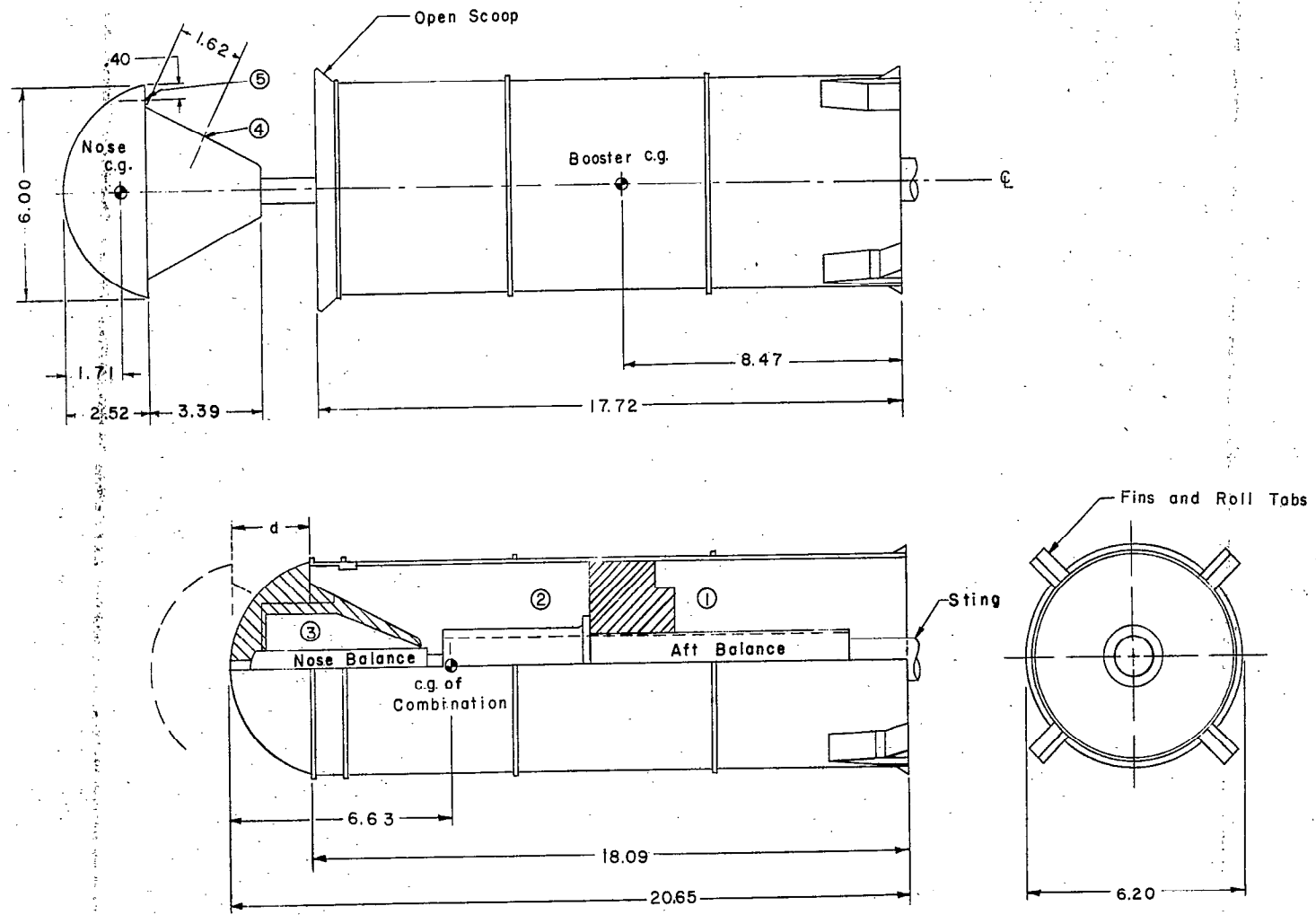
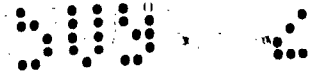
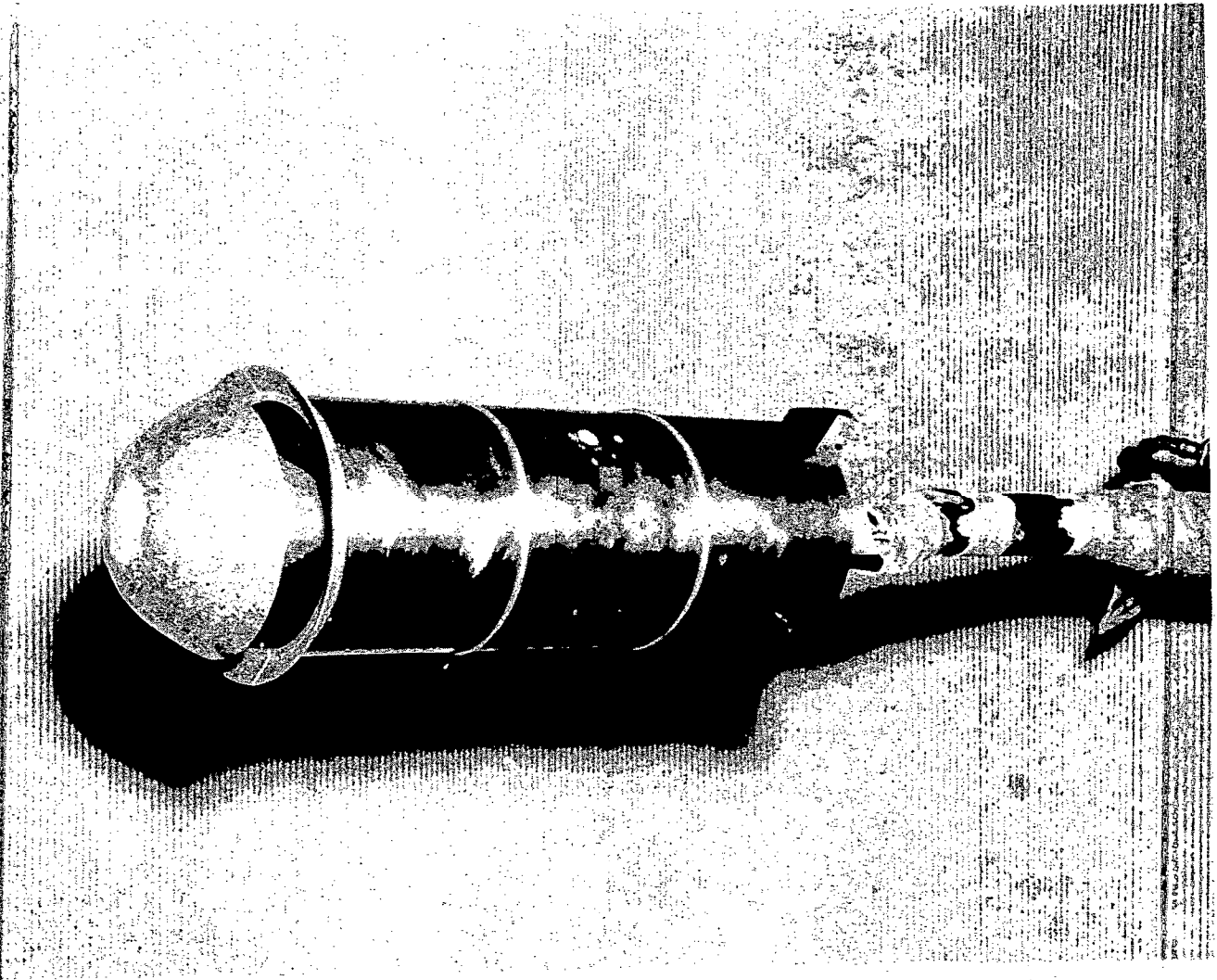


Figure 1.- Sketch of 1/10-scale model of the AVCO booster vehicle. All dimensions are in inches and the circled numbers indicate locations of static-pressure orifices. Vehicle is shown in  $\phi = 0^\circ$  position.



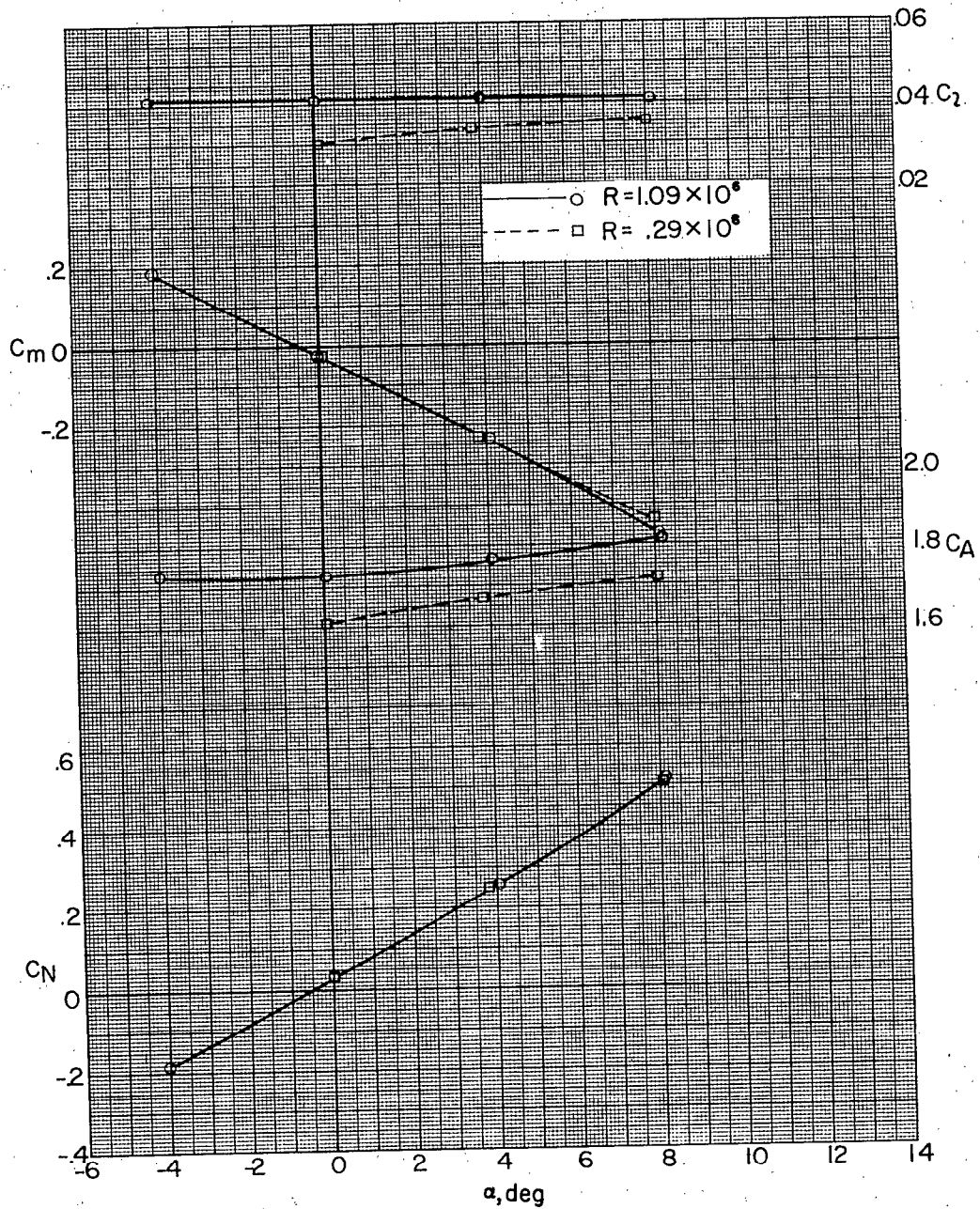
~~CONFIDENTIAL~~



~~CONFIDENTIAL~~

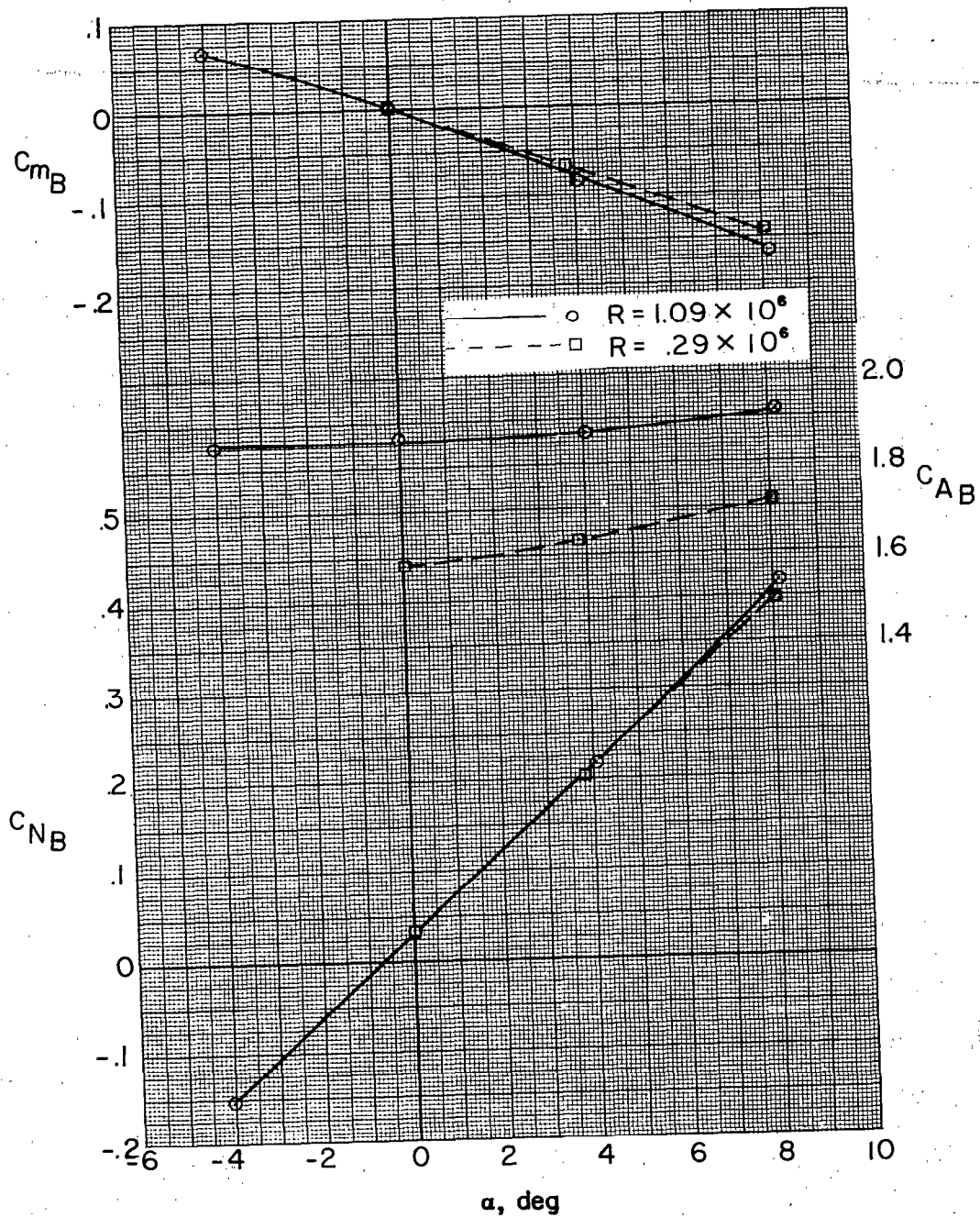
Figure 2.- One-tenth-scale model of the AVCO booster vehicle.

L-95588



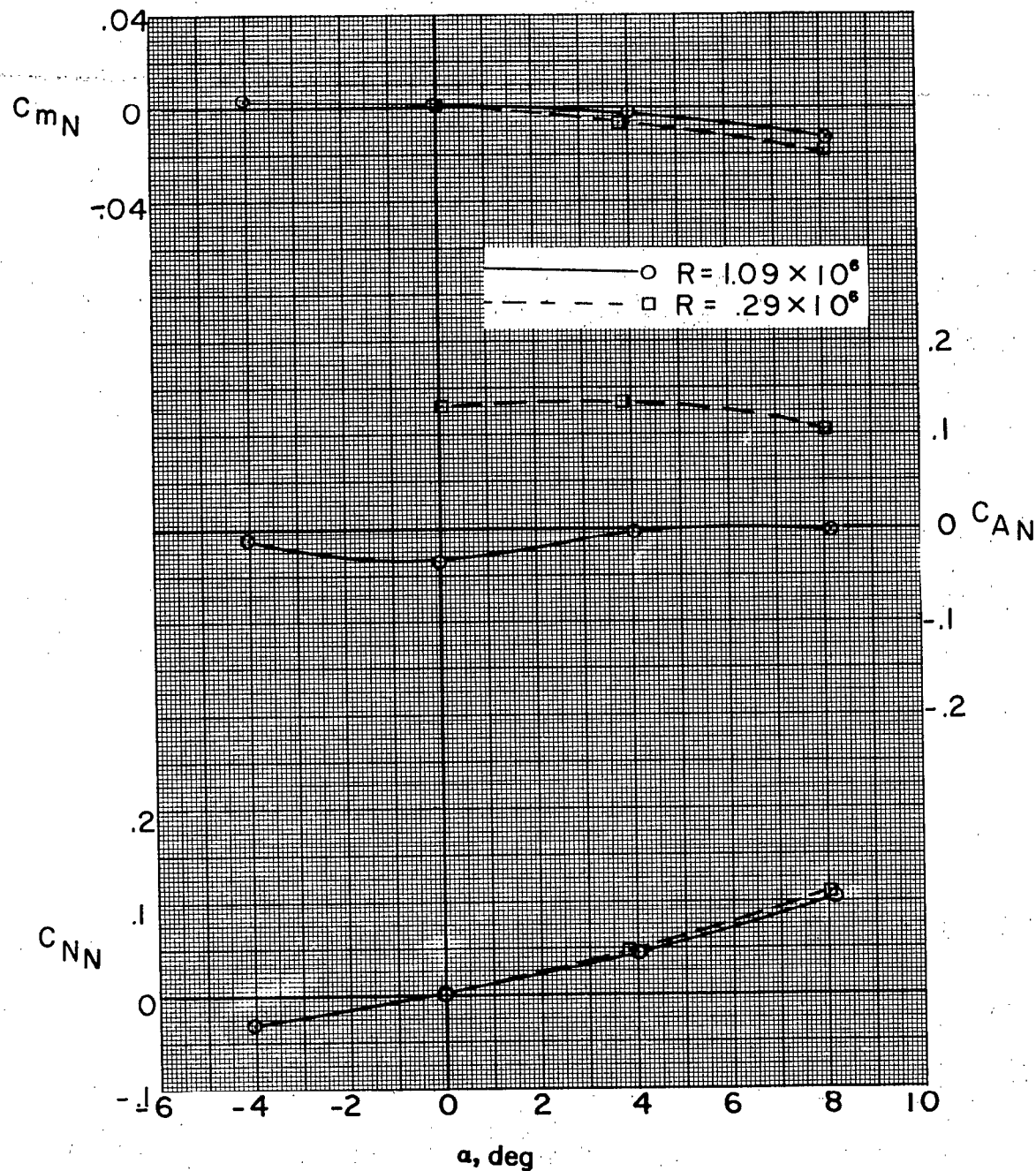
(a) Complete model.

Figure 3.- Effect of Reynolds number at  $M = 2.00$ ; open scoop,  $d = 0.04$  inch, and  $\phi = 0^\circ$ .



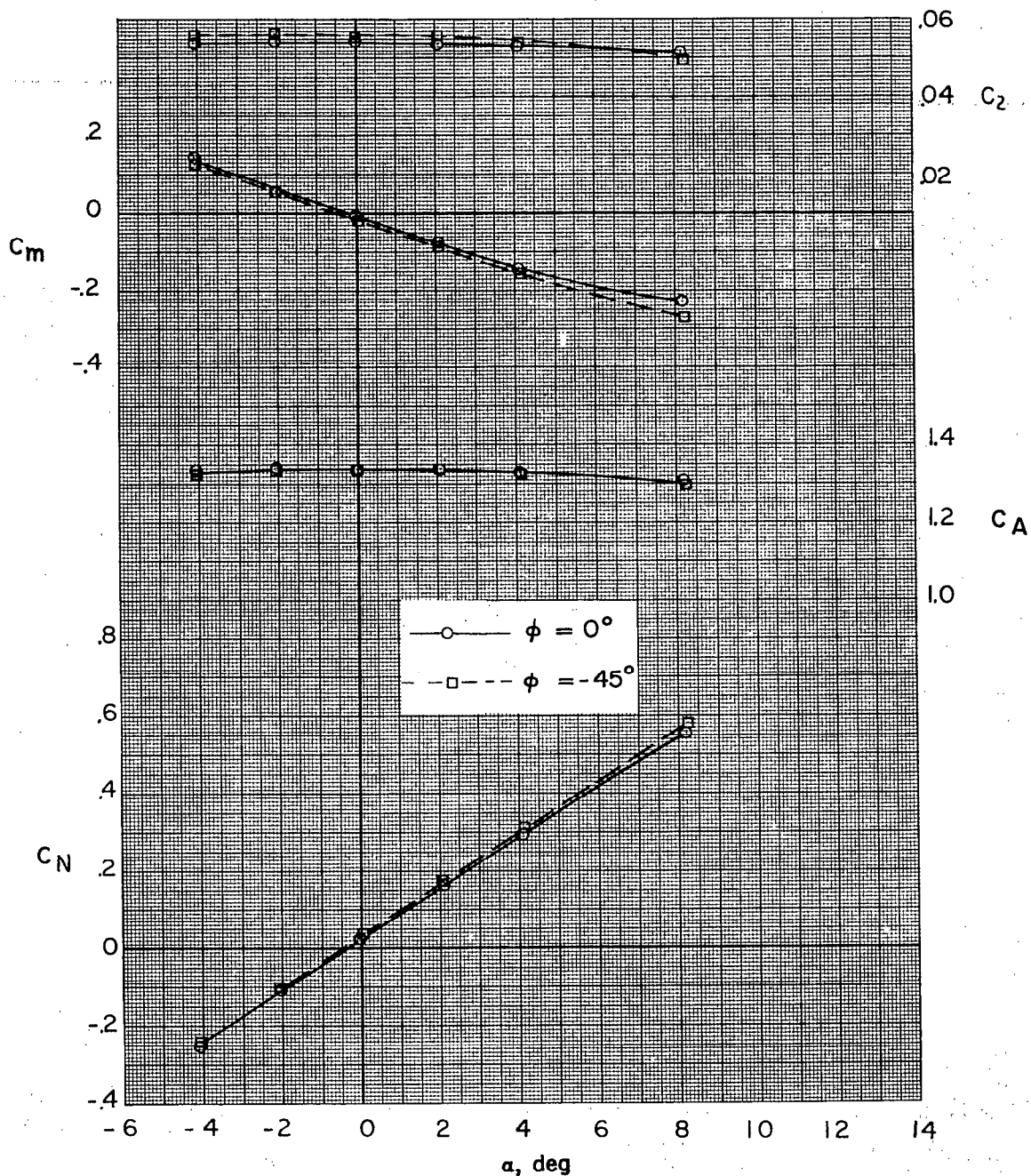
(b) Booster.

Figure 3.- Continued.



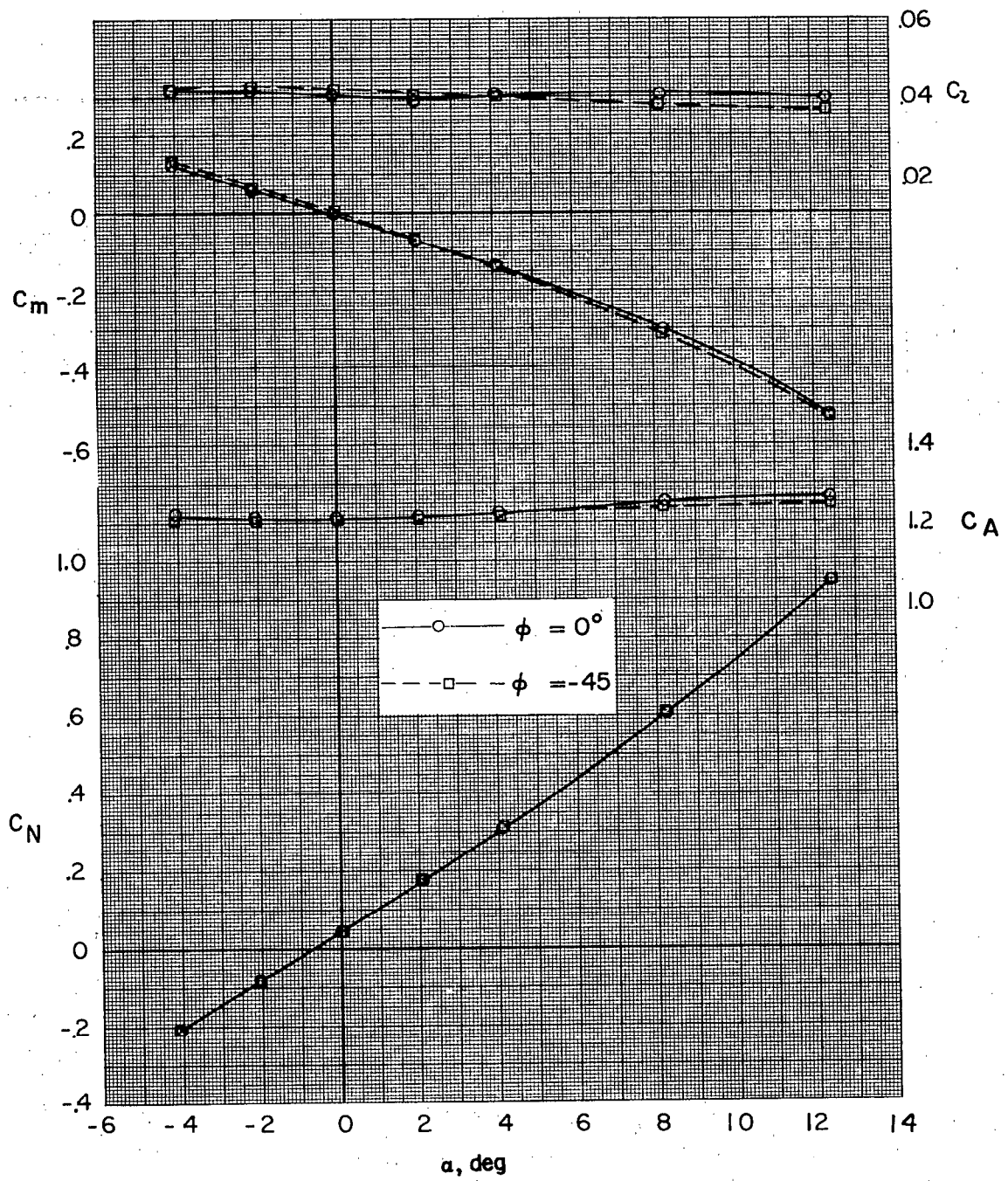
(c) Nose.

Figure 3.- Concluded.



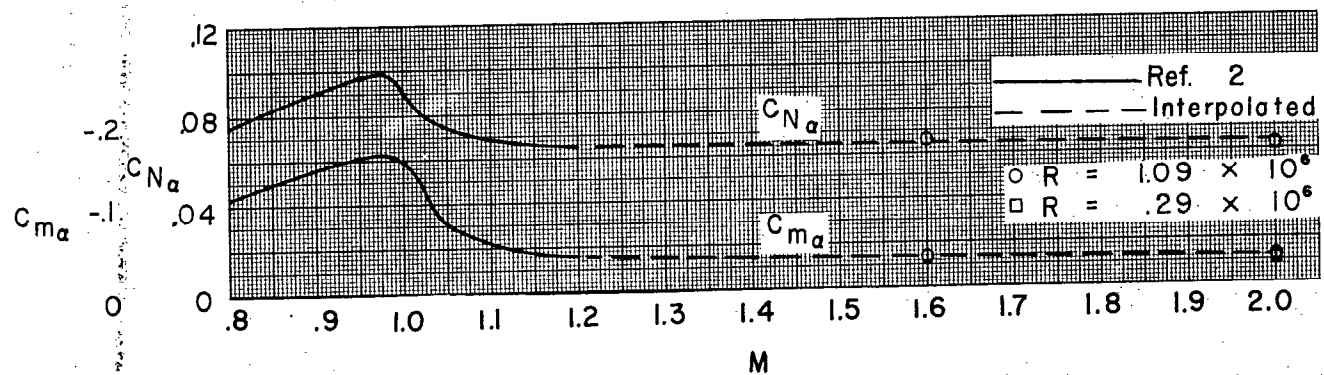
(a)  $M = 1.60$ .

Figure 4.- Effect of roll position of stabilizing fins for complete model; scoops closed and  $R = 1.09 \times 10^6$ .

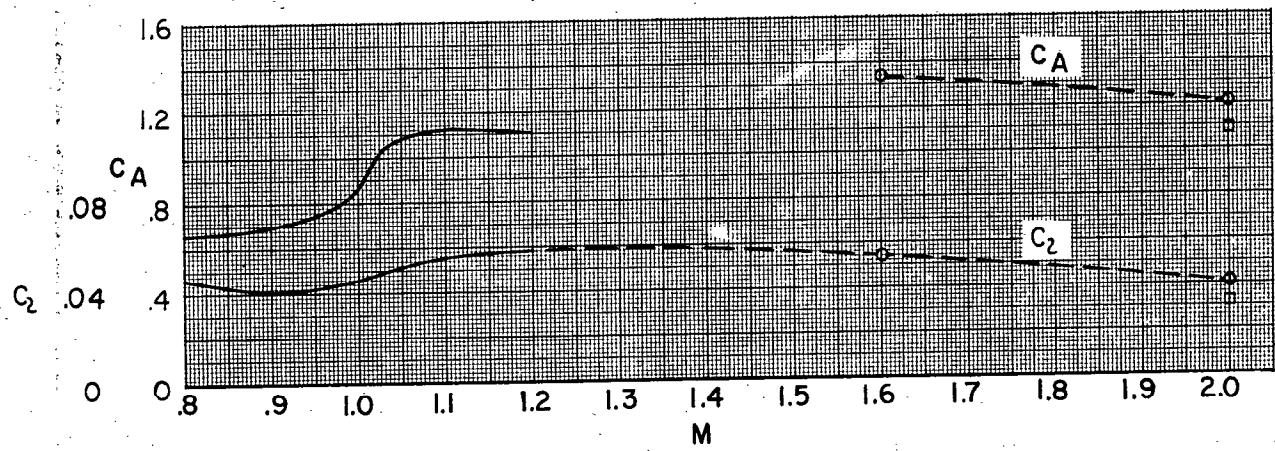


(b)  $M = 2.00$ .

Figure 4.- Concluded.

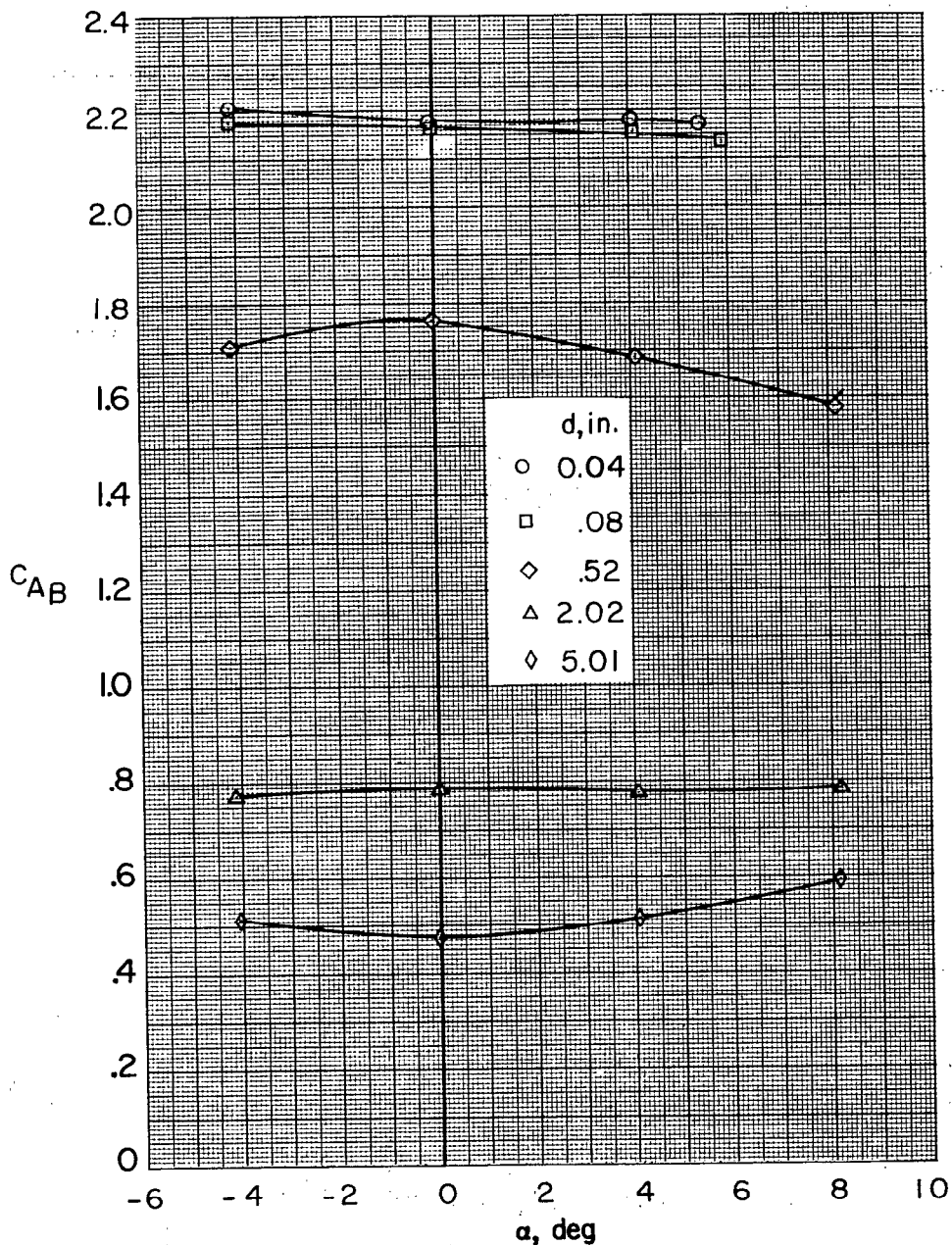


(a)  $C_{N_\alpha}$  and  $C_{m_\alpha}$ .



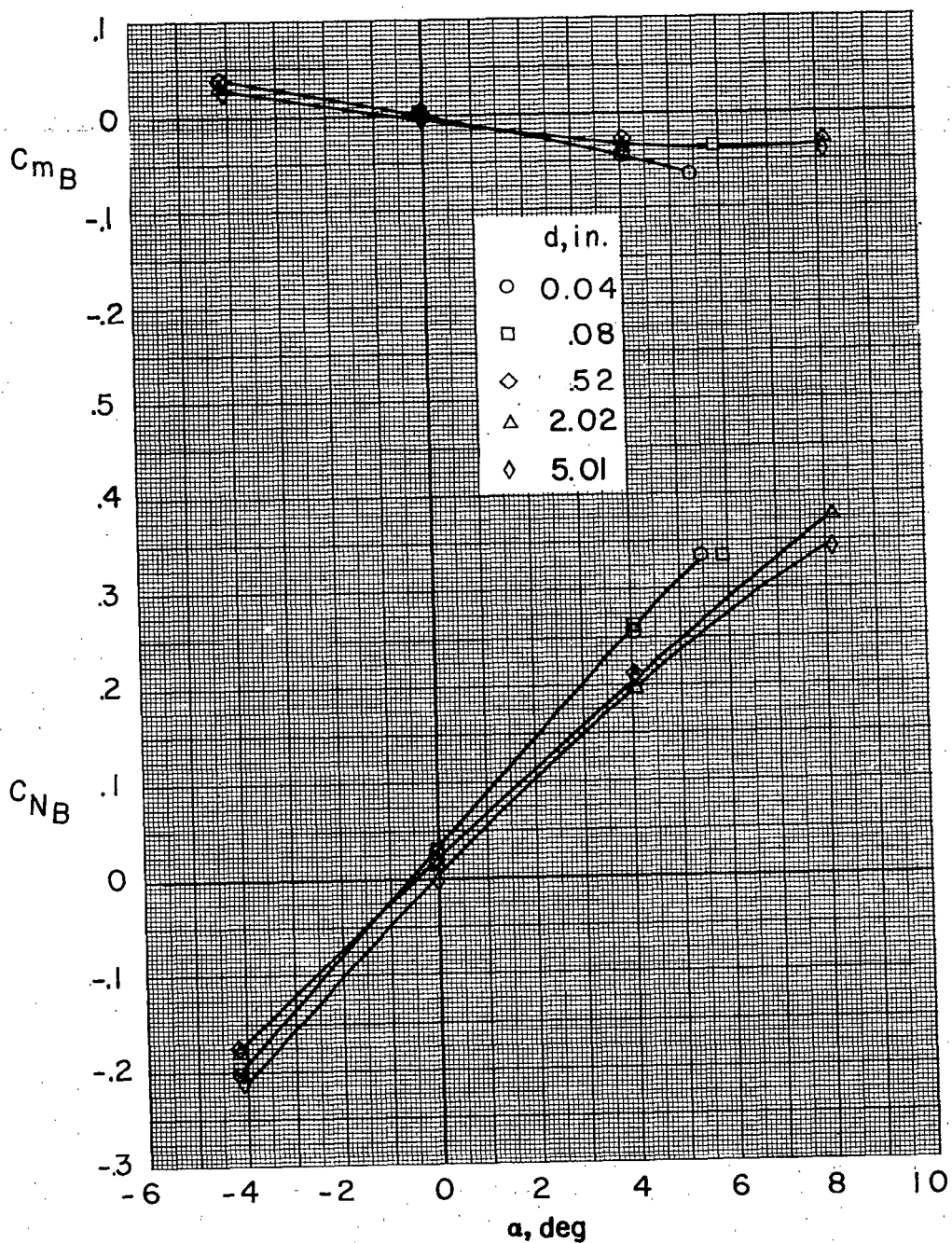
(b)  $C_A$  and  $C_z$  at  $\alpha = 0^\circ$ .

Figure 5.- Variation with Mach number of complete-model pitch characteristics; closed scoops and  $\phi = 0^\circ$ .



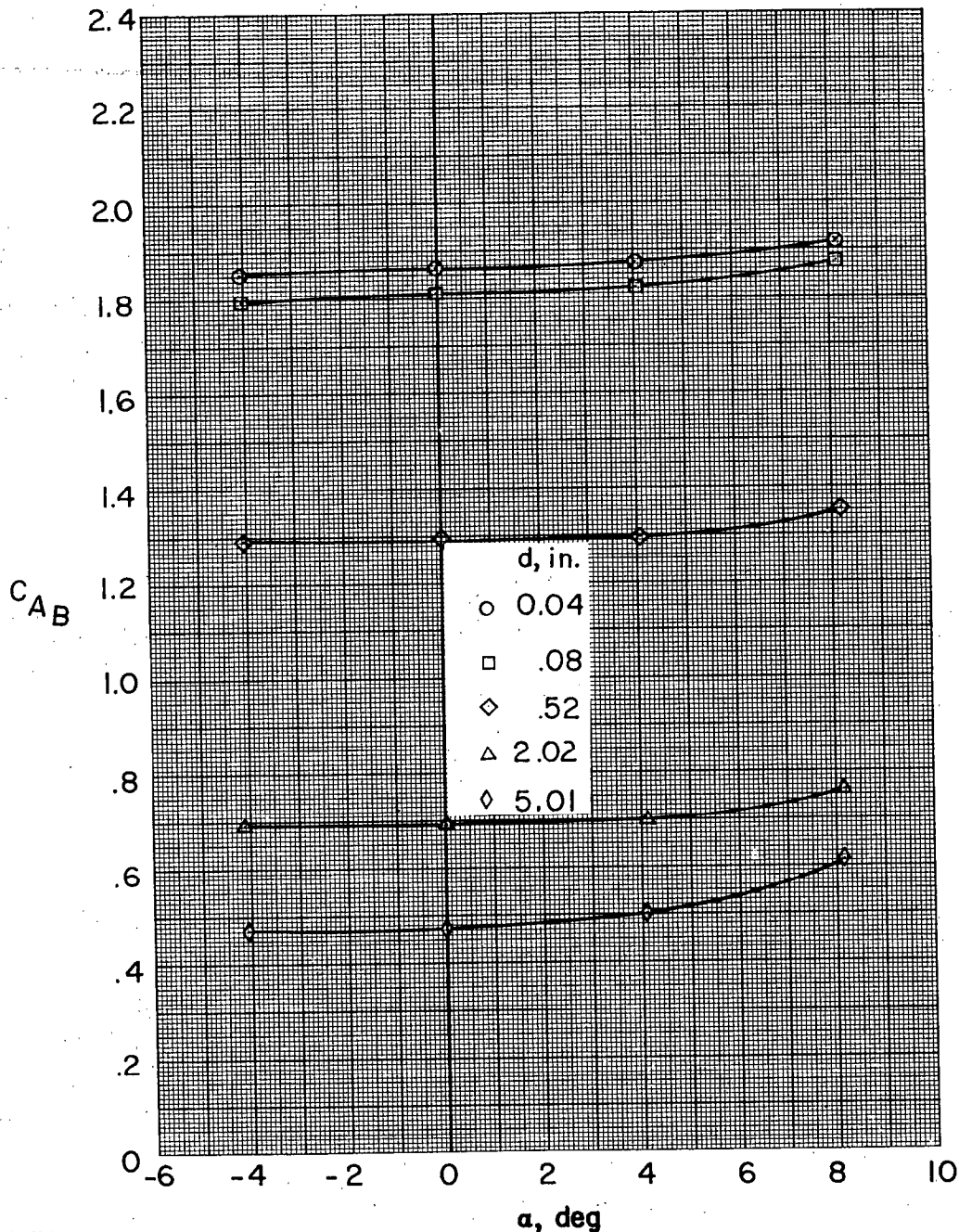
(a)  $M = 1.60$ .

Figure 6.- Effect of separation distance on booster characteristics; scoops open,  $\phi = 0^\circ$ , and  $R = 1.09 \times 10^6$ .



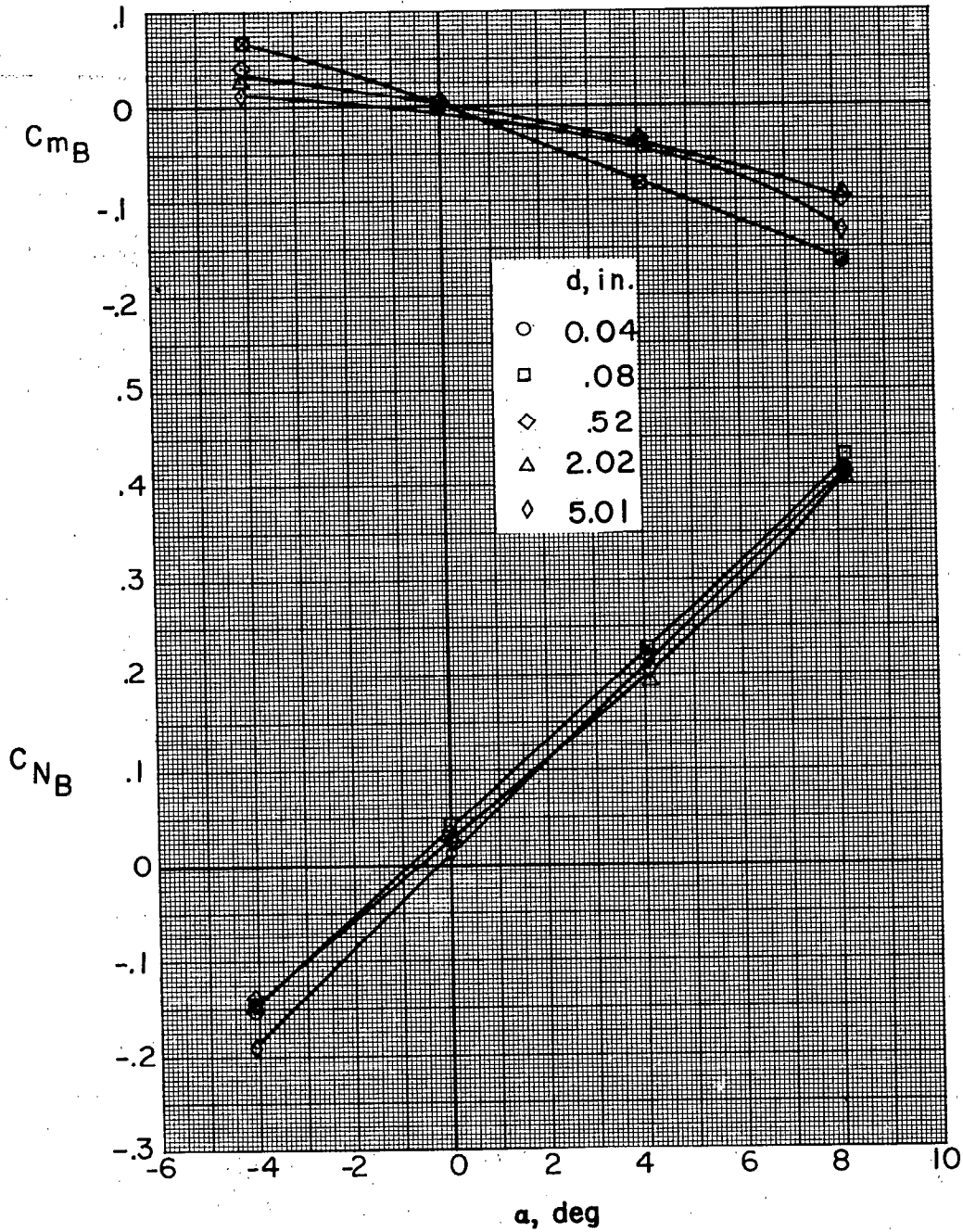
(a) Concluded.

Figure 6.- Continued.



(b)  $M = 2.00$ .

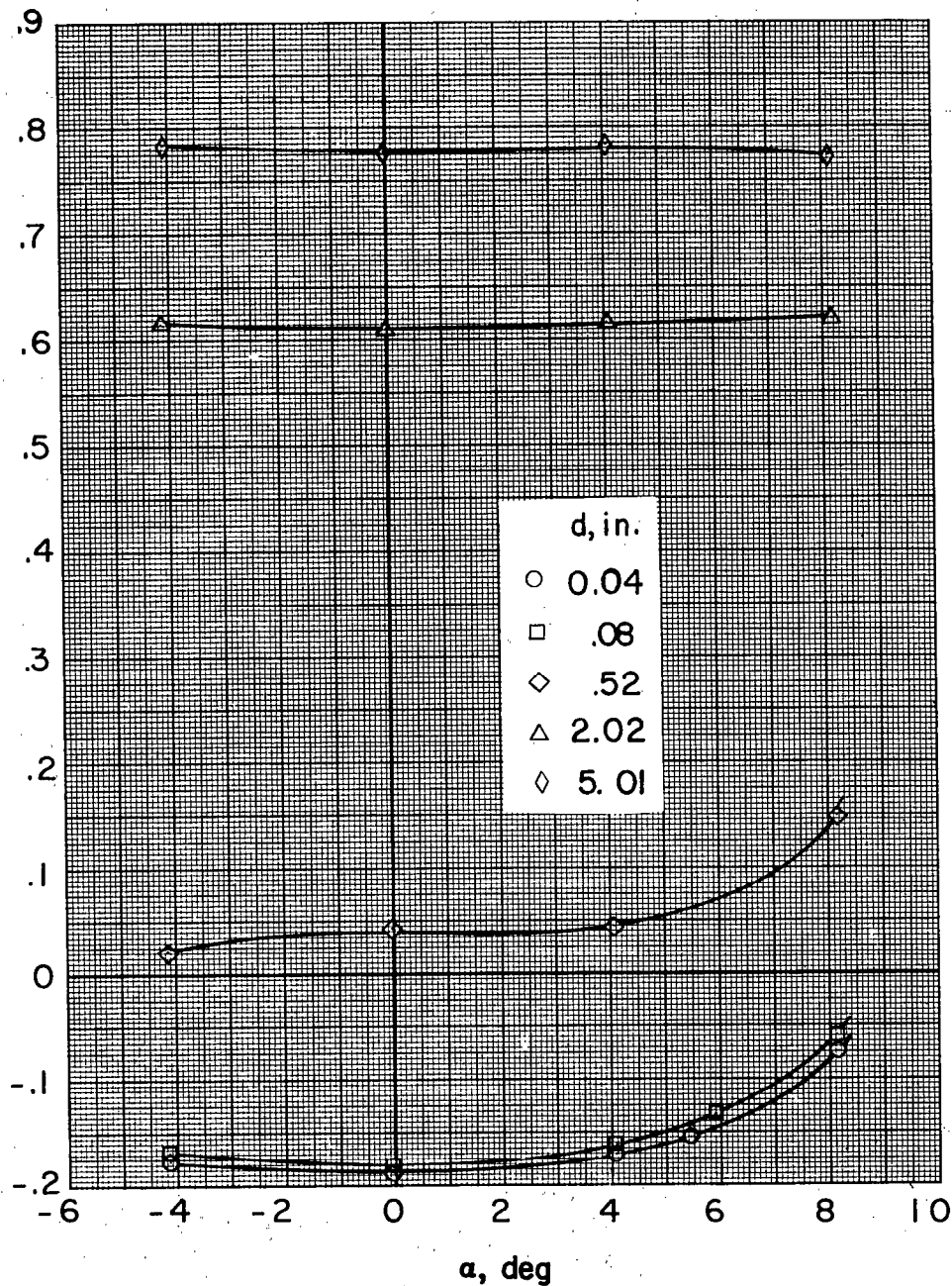
Figure 6.- Continued.



(b) Concluded.

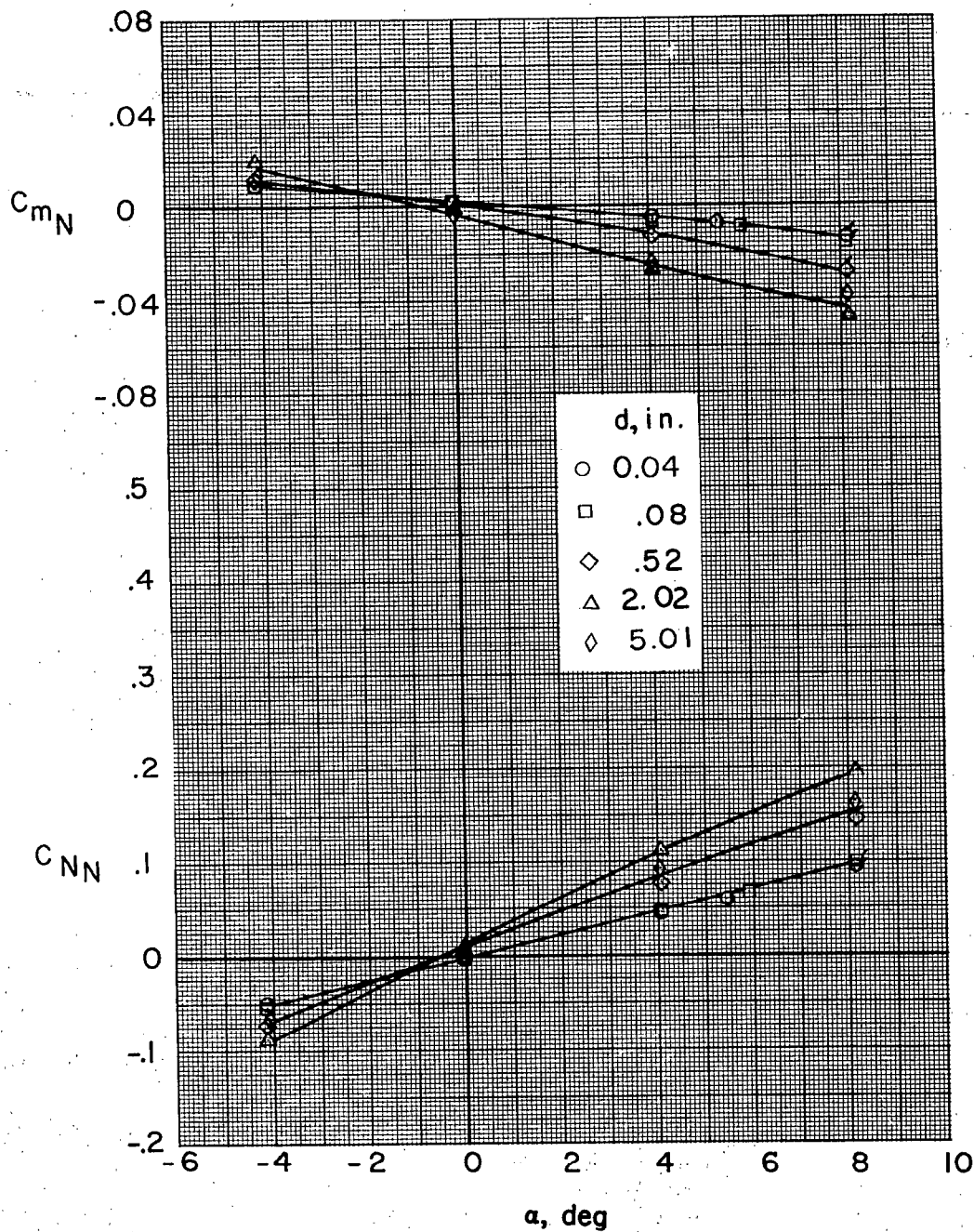
Figure 6.- Concluded.

CAN



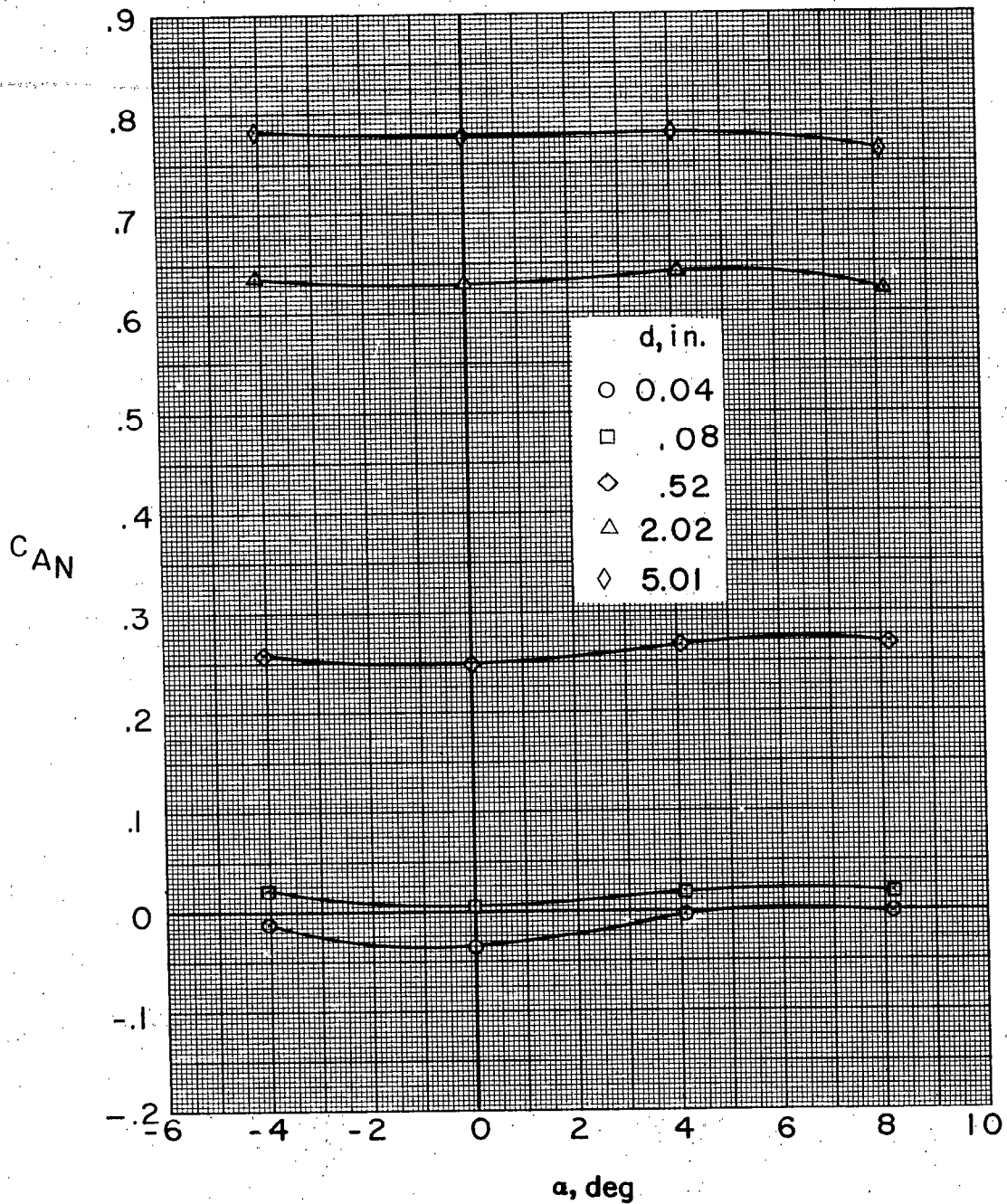
(a)  $M = 1.60$ .

Figure 7.- Effect of separation distance on nose characteristics; scoops open,  $\phi = 0^\circ$ , and  $R = 1.09 \times 10^6$ .



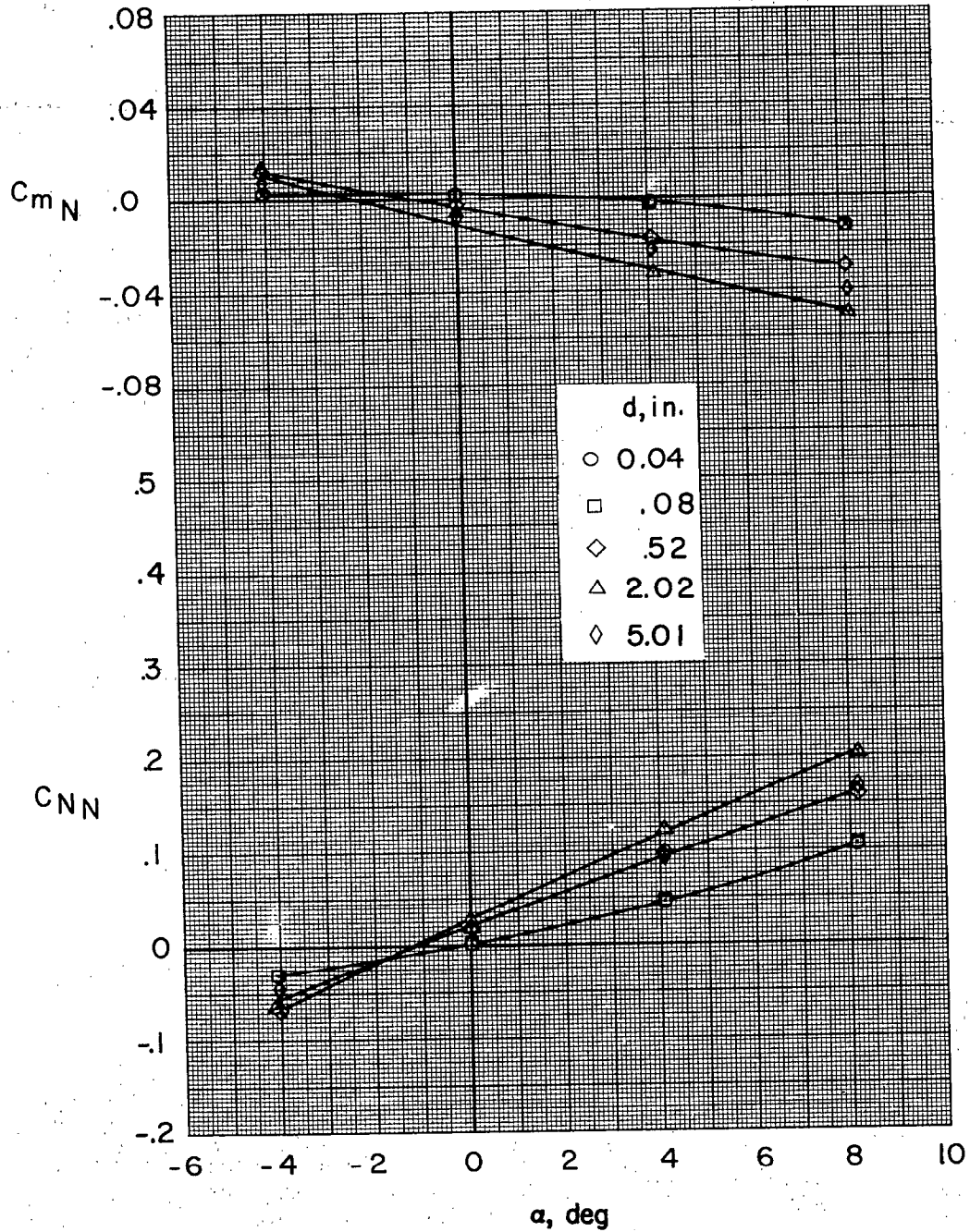
(a) Concluded.

Figure 7.- Continued.



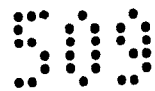
(b)  $M = 2.00$ .

Figure 7.- Continued.

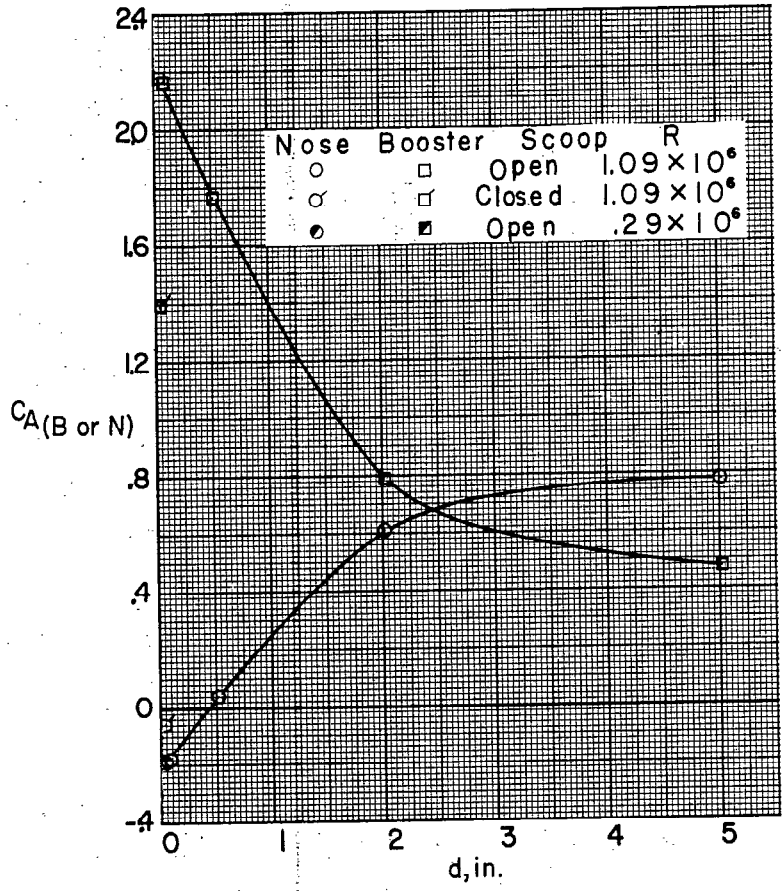


(b) Concluded.

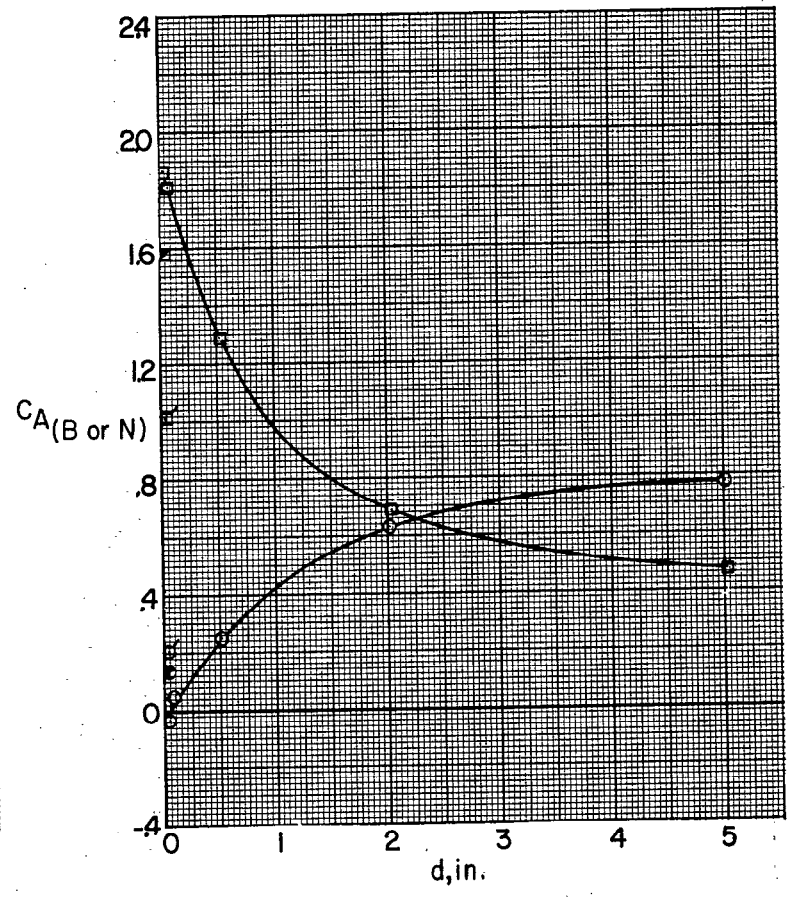
Figure 7.- Concluded.



CONFIDENTIAL

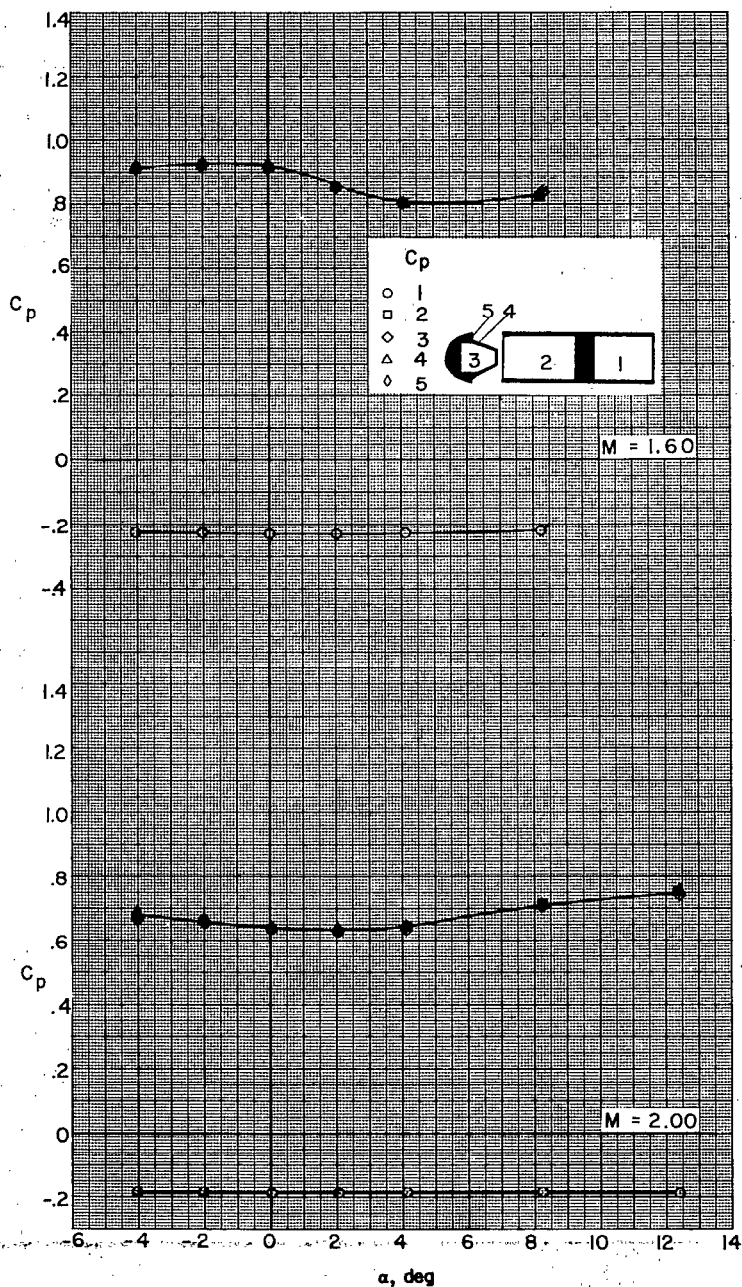


(a)  $M = 1.60$ .



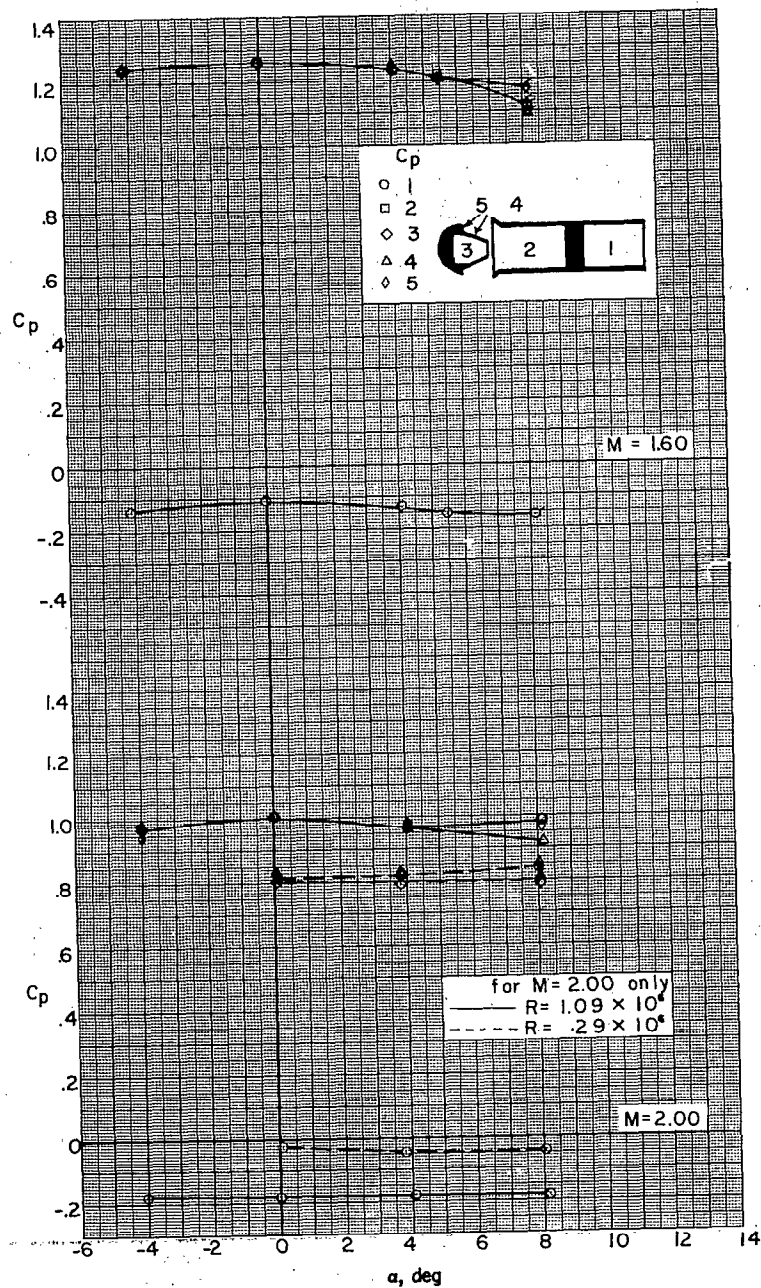
(b)  $M = 2.00$ .

Figure 8.- Variation with separation distance of zero-angle-of-attack axial-force coefficients,  $\phi = 0^\circ$ .



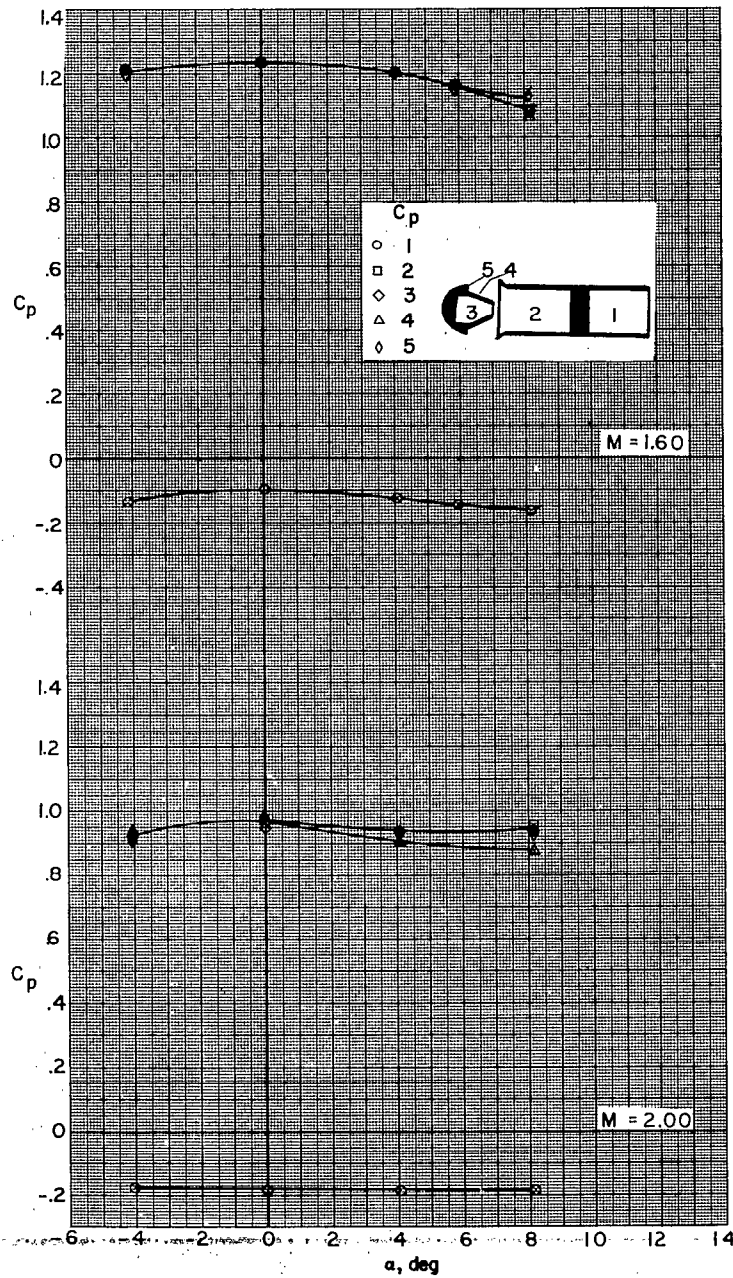
(a)  $d = 0.04$  inch; closed scoop.

Figure 9.- Variation with angle of attack of pressure coefficients;  
 $\phi = 0^\circ$  and  $R = 1.09 \times 10^6$ .



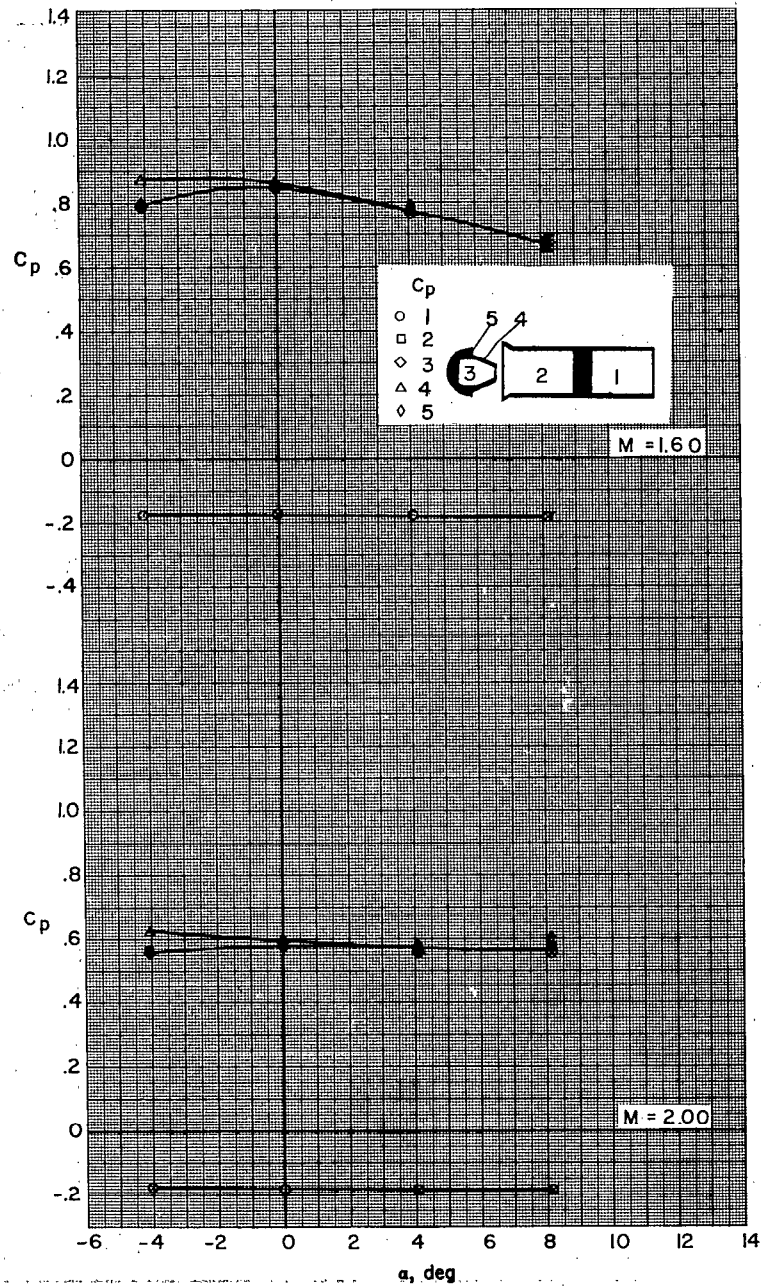
(b)  $d = 0.04$  inch; open scoop.

Figure 9.- Continued.



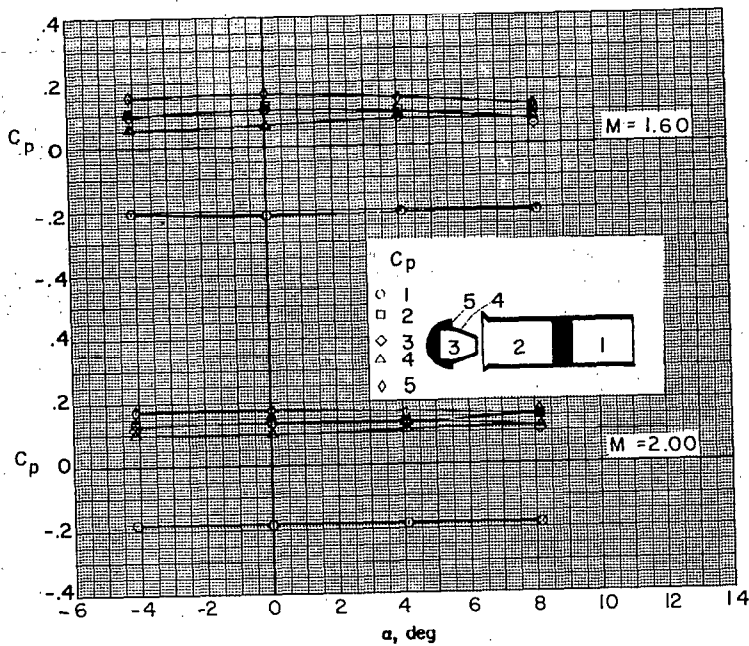
(c)  $d = 0.08$  inch; open scoop.

Figure 9.- Continued.

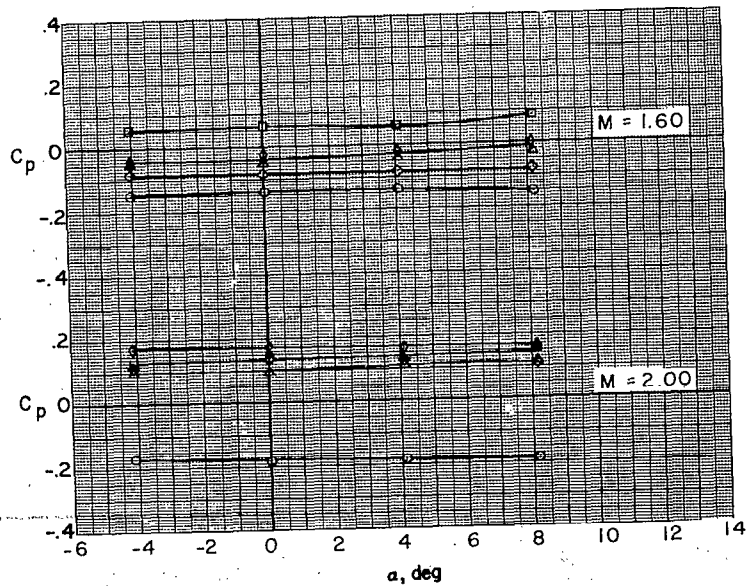


(d)  $d = 0.52$  inch; open scoop.

Figure 9.- Continued.

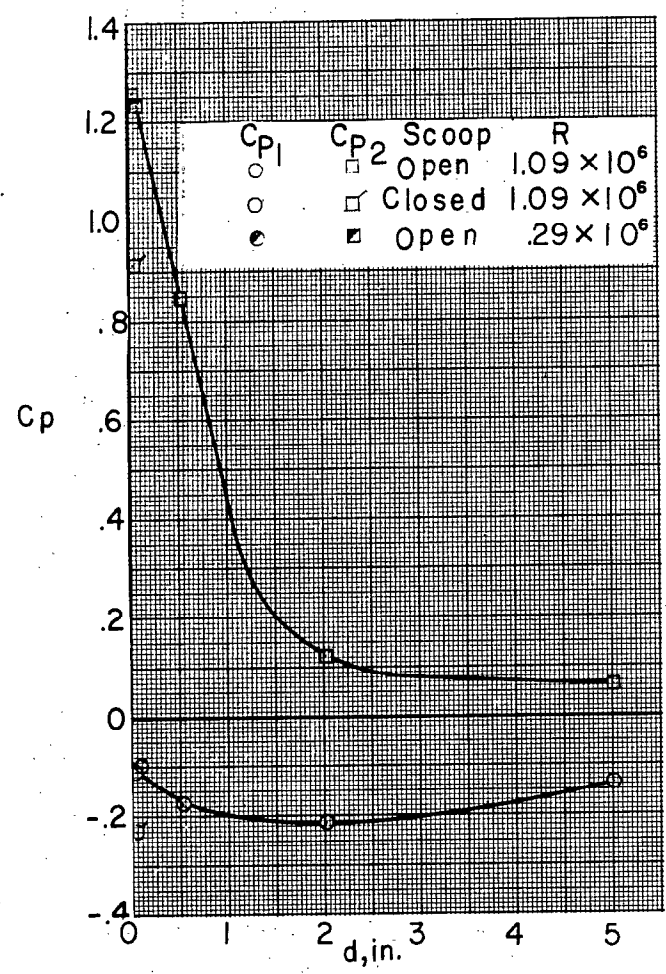


(e)  $d = 2.02$  inches; open scoop.

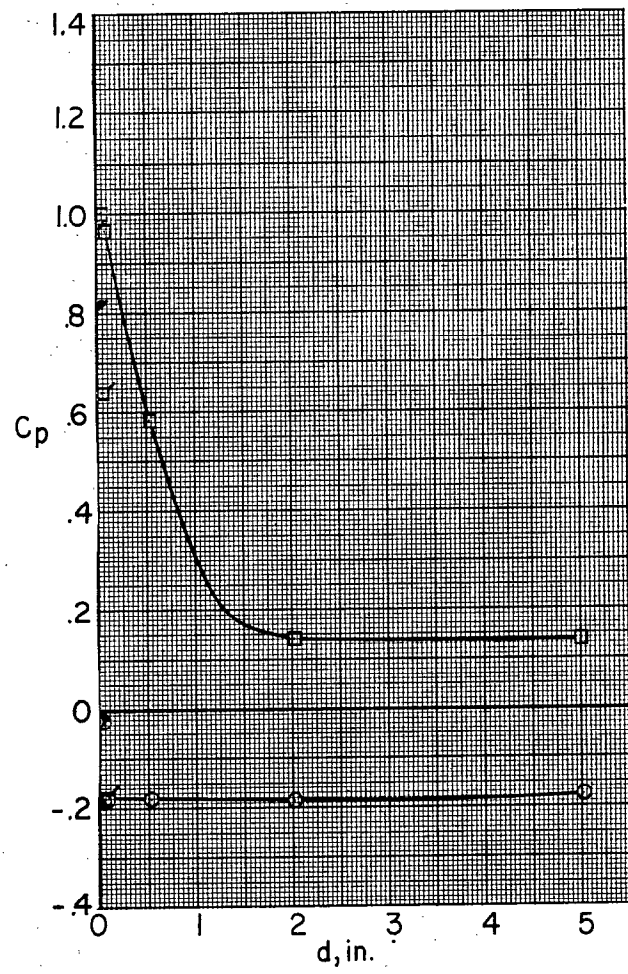


(f)  $d = 5.01$  inches; open scoop.

Figure 9.- Concluded.

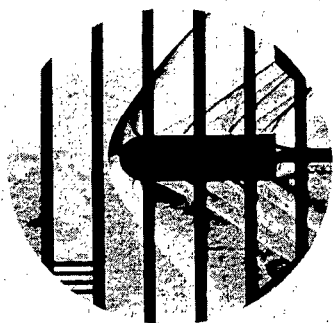


(a)  $M = 1.60$ .

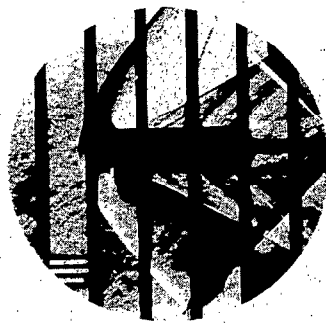


(b)  $M = 2.00$ .

Figure 10.- Variation of separation distance of zero-angle-of-attack pressure coefficients,  $\phi = 0^\circ$ .



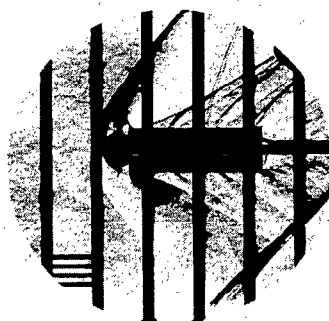
Closed Scoop



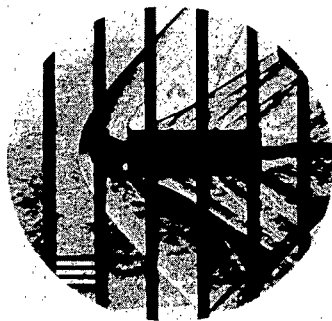
Open Scoop,  $d = .04$  in.



Open Scoop,  $d = .08$  in.



Open Scoop,  $d = .52$  in.



Open Scoop,  $d = 2.02$  in.



Open Scoop,  $d = 5.0$  in.

(a)  $M = 1.60.$

L-57-1569

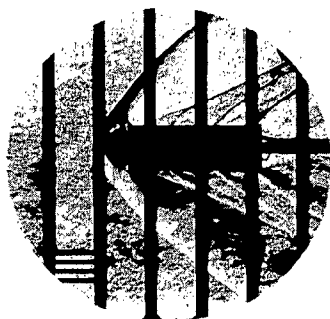
Figure 11.- Schlieren photographs of model at two Mach numbers.  $\alpha = 0^\circ;$   
 $\phi = 0^\circ.$



Closed Scoop



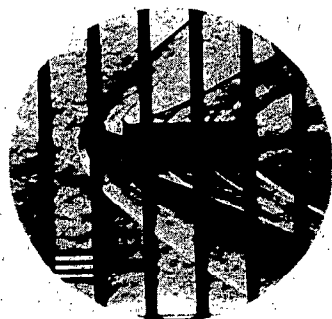
Open Scoop,  $d = .04$  in.



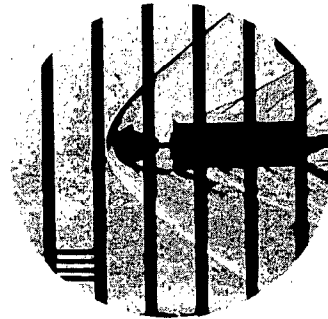
Open Scoop,  $d = .08$  in.



Open Scoop,  $d = .52$  in.



Open Scoop,  $d = 2.02$  in.



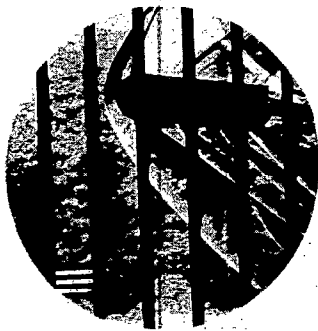
Open Scoop,  $d = 5.01$  in.

(b)  $M = 2.00.$

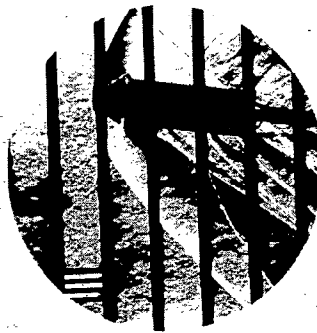
L-57-1570

Figure 11.- Concluded.

300



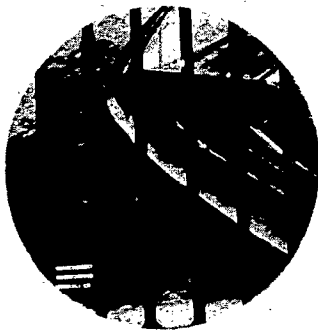
Closed Scoop



Open Scoop, d = .04 in.  
(a) M = 1.60.



Open Scoop, d = 2.02 in.



Closed Scoop



Open Scoop, d = .04 in.  
(b) M = 2.00.



Open Scoop, d = 2.02 in.

Figure 12.- Schlieren photographs of model at two Mach numbers.  $\alpha = 8^\circ$ ;  $\phi = 0^\circ$ . L-57-1571

CONFIDENTIAL

CONFIDENTIAL

INVESTIGATION OF STATIC STABILITY AND DRAG CHARACTERISTICS  
OF A 1/10-SCALE MODEL OF THE AVCO BOOSTER VEHICLE  
AT MACH NUMBERS OF 1.60 AND 2.00

COORD. NO. AF-AM-58

By James D. Church and Lawrence M. Sista

ABSTRACT

An investigation has been conducted in the Langley Unitary Plan wind tunnel to determine the static stability and drag characteristics of a 1/10-scale model of the AVCO booster vehicle. The tests were made at a constant Reynolds number, based on maximum nose diameter, of  $1.09 \times 10^6$  at Mach numbers of 1.60 and 2.00. Results were obtained for angles of attack from  $-4^\circ$  to  $12^\circ$  and for various separation distances of the nose from the booster. Also included are some effects of Reynolds number, roll position of the stabilizing fins, and booster drag scoops.

INDEX HEADINGS

Bodies	1.3
Missiles	1.7.2
Stability, Longitudinal - Static	1.8.1.1.1

NASA Technical Library



3 1176 01437 9292

